Updating neutrino magnetic moment constraints.

Phys. Lett. B753, 191 (2016)

Blanca Cecilia Cañas Orduz
O. G. Miranda, A. Parada, M. Tortola and J. W. F. Valle

Departamento de Física, CINVESTAV

XXX Reunión Anual de la División de Partículas y Campos
DPyC SMF

Outline

Electromagnetic interactions

In the Standard Model (SM)

$$\mathcal{H}^f_{em}(x) = j^f_\mu(x)A^\mu(x) = \mathfrak{q}_f \bar{f}(x)\gamma_\mu f(x)A^\mu(x),$$

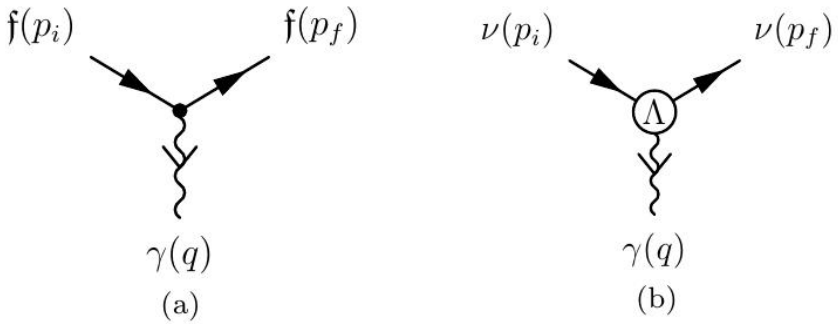

Figure 1: Tree-level coupling of a charged fermion f with a photon γ (a) and effective one-photon coupling of a neutrino with a photon (b).

* For neutrinos: $q_\nu = 0 \rightarrow$ there are no electromagnetic interactions at tree level.

* However, such interactions can arise from loop diagrams at higher order in the perturbative expansion.

$$\mathcal{H}_{eff}(x) = j^{eff}_\mu(x)A^\mu(x) = \bar{\nu}(x)\Lambda_\mu\nu(x)A^\mu(x).$$

Majorana neutrinos

If Majorana neutrinos are furnished with magnetic moments (MM) and electric dipole moments (EDM), the interaction with the electromagnetic field is described by the effective Hamiltonian [1]

$$\mathcal{H}^M_{em} = -\frac{1}{4}\nu^T C^{-1}\left(\mu + i d\gamma_5\right)\sigma^{\alpha\beta}\nu F_{\alpha\beta} = -\frac{1}{4}\nu_L^T C^{-1}\,\lambda\,\sigma^{\alpha\beta}\nu_L F_{\alpha\beta} + h.c.,$$

with $\nu = \nu_L + (\nu_L)^c$ and C is the charge conjugation matrix.

$$\mu^T = -\mu \quad \text{(MM matrix)}, \qquad d^T = -d \quad \text{(EDM matrix)}.$$

The MM and EDM matrices are condensed in $\lambda = \mu - id$ (NMM matrix).

The MM and EDM matrices are antisymmetric and hermitian, and, therefore, imaginary. λ is an antisymmetric matrix.

[1] J. Schechter and J. W. F. Valle, Phys. Rev. D24, 1883 (1981)

The above discussion could be translated into a more phenomenological approach in which the Dirac NMM is described by a complex matrix $\lambda = \mu - id\ (\tilde{\lambda})$ in the flavor (mass) basis, while for the Majorana case the matrix λ takes the form

$$\lambda = \begin{pmatrix} 0 & \Lambda_\tau & -\Lambda_\mu \\ -\Lambda_\tau & 0 & \Lambda_e \\ \Lambda_\mu & -\Lambda_e & 0 \end{pmatrix}, \qquad \tilde{\lambda} = \begin{pmatrix} 0 & \Lambda_3 & -\Lambda_2 \\ -\Lambda_3 & 0 & \Lambda_1 \\ \Lambda_2 & -\Lambda_1 & 0 \end{pmatrix},$$

where $\lambda_{\alpha\beta} = \varepsilon_{\alpha\beta\gamma}\Lambda_\gamma$.

The transition magnetic moments Λ_α and Λ_i are complex parameters:

$$\Lambda_\alpha = |\Lambda_\alpha| e^{i\zeta_\alpha}, \qquad \Lambda_i = |\Lambda_i| e^{i\zeta_i}.$$

Neutrino-electron elastic scattering

$$\left(\frac{d\sigma}{dT}\right)(\nu + e^- \to \nu + e^-) = \left(\frac{d\sigma}{dT}\right)_{SM} + \left(\frac{d\sigma}{dT}\right)_{em}.$$

The SM contribution is

$$\left(\frac{d\sigma}{dT}\right)_{SM} = \frac{G_F^2 m_e}{2\pi}\left[(g_V + g_A)^2 + (g_V - g_A)^2\left(1 - \frac{T}{E_\nu}\right)^2 + (g_A^2 - g_V^2)\frac{m_e T}{E_\nu^2}\right],$$

where

$$g_V = \begin{cases} 2\sin^2\theta_W + \frac{1}{2} & \text{for} \quad \nu_e \\ 2\sin^2\theta_W - \frac{1}{2} & \text{for} \quad \nu_\mu, \nu_\tau \end{cases} \qquad g_A = \begin{cases} \frac{1}{2} & \text{for} \quad \nu_e \\ -\frac{1}{2} & \text{for} \quad \nu_\mu, \nu_\tau \end{cases}$$

with $g_A \to -g_A \Longrightarrow (\bar{\nu_e}, \bar{\nu_\mu}, \bar{\nu_\tau})$.

The electromagnetic contribution is given by

$$\left(\frac{d\sigma}{dT}\right)_{em} = \frac{\pi\alpha^2}{m_e^2\mu_B^2}\left(\frac{1}{T} - \frac{1}{E_\nu}\right)\mu_\nu{}^2,$$

where μ_ν is an effective magnetic moment.

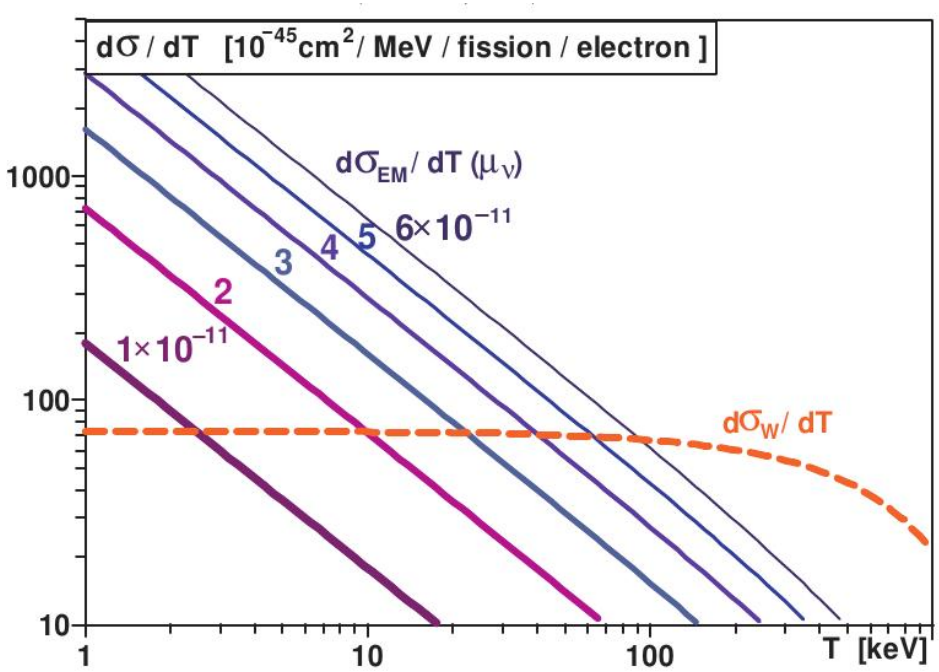

Figure 2: Weak and electromagnetic cross-sections calculated for several neutrino magnetic moment values.

μ_ν is defined in the flavor basis as [2]

$$(\mu_\nu^F)^2 = a_-^\dagger \lambda^\dagger \lambda a_- + a_+^\dagger \lambda \lambda^\dagger a_+,$$

where a_- and a_+ denote the negative and positive helicity neutrino, respectively. Whereas, in the mass basis

$$(\mu_\nu^M)^2 = \tilde{a}_-^\dagger \tilde{\lambda}^\dagger \tilde{\lambda} \tilde{a}_- + \tilde{a}_+^\dagger \tilde{\lambda} \tilde{\lambda}^\dagger \tilde{a}_+.$$

$\tilde{a}_- = U^\dagger a_-, \qquad \tilde{a}_+ = U^T a_+, \qquad \tilde{\lambda} = U^T \lambda U.$

$$\tilde{\lambda} \rightarrow 3 \text{ MM phases} \quad \rightarrow \quad \zeta_1, \zeta_2, \zeta_3 \quad (\Lambda_i = |\Lambda_i| e^{i\zeta_i})$$

$$U \rightarrow 3 \text{ CPV phases} \quad \rightarrow \quad \delta, \quad 2 - \text{Majorana phases},$$

three of these six complex phases are irrelevant, as they can be reabsorbed in different ways [3].

We give our results in terms of: δ, $\xi_2 = \zeta_3 - \zeta_1$ and $\xi_3 = \zeta_2 - \zeta_1$.

[2] W. Grimus, T. Schwetz, Nucl Phys. B 587 (2000) 45; W. Grimus, et al., Nucl Phys. B 648 (2003) 376.

[3] Grimus et al

Effective NMM at reactor experiments.

In the flavor basis

$$(\mu_\nu^F)^2 = a_-^\dagger \lambda^\dagger \lambda a_- + a_+^\dagger \lambda \lambda^\dagger a_+.$$

In this case ($\overline{\nu_e}$): a_+^T=(1,0,0), a_-^T=(0,0,0).

$$(\mu_R^F)^2 = |\Lambda_\mu|^2 + |\Lambda_\tau|^2.$$

In the mass basis

$$\begin{aligned}(\mu_R^M)^2 &= |\mathbf{\Lambda}|^2 - s_{12}^2 c_{13}^2 |\Lambda_2|^2 - c_{12}^2 c_{13}^2 |\Lambda_1|^2 - s_{13}^2 |\Lambda_3|^2 \\ &- 2 s_{12} c_{12} c_{13}^2 |\Lambda_1||\Lambda_2| \cos\delta_{12} - 2 c_{12} c_{13} s_{13} |\Lambda_1||\Lambda_3| \cos\delta_{13} \\ &- 2 s_{12} c_{13} s_{13} |\Lambda_2||\Lambda_3| \cos\delta_{23}, \qquad \theta_{13} \neq 0\end{aligned}$$

$\delta_{12} = \xi_3$, $\delta_{23} = \xi_2 - \delta$, and $\delta_{13} = \delta_{12} - \delta_{23}$.

Effective NMM at acelerator experiments.

$$(\mu_\nu^F)^2 = a_-^\dagger \lambda^\dagger \lambda a_- + a_+^\dagger \lambda \lambda^\dagger a_+.$$

In this case $(\overline{\nu_\mu}, \nu_e, \nu_\mu)$: a_+^T=(0,1,0), a_-^T=(1,1,0).

$$(\mu_A^F)^2 = |\mathbf{\Lambda}|^2 + |\Lambda_e|^2 + 2\,|\Lambda_\tau|^2 - 2\,|\Lambda_\mu||\Lambda_e|\cos\eta,$$

where $|\mathbf{\Lambda}|^2 = |\Lambda_e|^2 + |\Lambda_\mu|^2 + |\Lambda_\tau|^2$ and $\eta = \zeta_e - \zeta_\mu$.

Effective NMM at acelerator experiments.

In the mass basis, with $\theta_{13} \neq 0$.

$$
\begin{aligned}
(\mu_A^M)^2 &= |\Lambda_1|^2 \left[\sin 2\theta_{12} c_{13} c_{23} + c_{12}^2 (2c_{23}^2 + \sin 2\theta_{13} s_{23} \cos\delta)\right. \\
&+ \left. c_{13}^2 (s_{12}^2 + 2s_{23}^2) + s_{13}(s_{13} + 2s_{12}^2 s_{13} s_{23}^2 - \sin 2\theta_{12} \sin 2\theta_{23} \cos\delta)\right] \\
&+ \frac{1}{4}|\Lambda_2|^2 \left[8 - \cos 2\theta_{23}(1 + 3\cos 2\theta_{12} + 2\cos 2\theta_{13} s_{12}^2) + 4 s_{12}^2 \sin 2\theta_{13} s_{23} \cos\delta\right. \\
&+ \left. 4 \sin 2\theta_{12}(-c_{13} c_{23} + s_{13} \sin 2\theta_{23} \cos\delta)\right] + |\Lambda_3|^2 \left(2 + c_{13}^2 \cos 2\theta_{23} - \sin 2\theta_{13} s_{23} \cos\delta\right) \\
&+ 2|\Lambda_1||\Lambda_2| \left\{\cos\xi_3 \left[-c_{12}^2 c_{13} c_{23} + c_{23}(s_{12}^2 c_{13} + \sin 2\theta_{12} c_{23})\right.\right. \\
&+ \left. s_{12} c_{12}(-1 + \cos 2\theta_{23} s_{13}^2 + \sin 2\theta_{13} s_{23} \cos\delta)\right] \\
&+ \left. s_{13} \sin 2\theta_{23}(\cos 2\theta_{12} \cos\delta \cos\xi_3 + \sin\delta \sin\xi_3)\right\} \\
&+ |\Lambda_1||\Lambda_3| \left\{2\cos(\xi_2 - \delta)(-c_{12} c_{13} \cos 2\theta_{23} + s_{12} c_{23}) s_{13}\right. \\
&+ \left. 2\left[c_{13} \cos\xi_2 (-c_{12} c_{13} + 2 s_{12} c_{23}) + c_{12} s_{13}^2 \cos(\xi_2 - 2\delta)\right] s_{23}\right\} \\
&- 2|\Lambda_2||\Lambda_3| \left\{\frac{1}{2} s_{12} \cos(\xi_1 - \delta)(\cos 2\theta_{23} \sin 2\theta_{13} + 2\cos 2\theta_{13} s_{23} \cos\delta)\right. \\
&+ \left. c_{12}\left[c_{23} s_{13} \cos(\xi_1 - \delta) + c_{13} \sin 2\theta_{23} \cos\xi_1\right] + s_{12} s_{23} \sin\delta \sin(\delta - \xi_1)\right\}.
\end{aligned}
$$

Effective neutrino magnetic moment in Borexino.

$$(\mu_\nu^M)^2 = \tilde{a}_-^\dagger \tilde{\lambda}^\dagger \tilde{\lambda} \tilde{a}_- + \tilde{a}_+^\dagger \tilde{\lambda} \tilde{\lambda}^\dagger \tilde{a}_+.$$

In this case

$$(\mu_{\rm sol}^M)^2 = |\mathbf{\Lambda}|^2 - c_{13}^2 |\Lambda_2|^2 + (c_{13}^2 - 1)|\Lambda_3|^2 + c_{13}^2 P_{e1}^{2\nu}(|\Lambda_2|^2 - |\Lambda_1|^2).$$

This expression is independent of any phase and we take into account the non-zero value of θ_{13} for the first time in this kind of analysis.

Neutrino data analysis: Reactor antineutrinos.

The total number of events (in the i-th bin) in these experiments is given by

$$N_R^i = \kappa \int dE_\nu \int dT \int_{T_i}^{T_{i+1}} dT' \lambda(E_\nu) \frac{d\sigma}{dT}(E_\nu, T, \mu) R(T, T').$$

The antineutrino energy spectrum coming from the nuclear reactor is [4]

$$\lambda(E_\nu) = \exp\left[\sum_{k=1}^{6} \alpha_{k\ell} E_\nu^{k-1}\right],$$

and the resolution function is given by

$$R(T, T') = \frac{1}{\sqrt{4\pi}\sigma} \exp\left(\frac{-(T - T')^2}{2\sigma^2}\right),$$

where σ stands for the error in the kinetic energy determination.

[4] T. Mueller, et al., Phys. Rev. C 83 (2011) 0.54615; V. Kopeikin, et al., Phys. At. Nucl. 60 (1997) 172.

Reactor antineutrinos.

Finally, we perform our statistical analysis using the following χ^2 function:

$$\chi^2 = \sum_{i=1}^{N_{bin}} \left(\frac{O_R^i - N_R^i(\mu_R)}{\Delta_i} \right)^2 ,$$

$O_R^i \longrightarrow$ the observed number of events

$N_R^i \longrightarrow$ the predicted number of events in the presence of an effective magnetic moment μ_R at the i-th bin.

$\Delta_i \longrightarrow$ the statistical error at each bin.

In our analysis, we have used the experimental results reported by Krasnoyarsk [5], Rovno [6], MUNU [7], and TEXONO [8] reactor experiments.

[5] G. Vidyakin, et al., JETP Lett. 55 (1992) 206.

[6] A.I. Derbin, et al., JETP Lett. 57 (1993) 768.

[7] Z. Daraktchieva, et al., Phys. Lett. B 615 (2005) 153.

[8] M. Deniz, et al., Phys. Rev. D 81 (2010) 072001.

Limits on the effective NMM from reactor and accelerator data

Experiment	Bounds
Reactors	
KRASNOYARSK	$\mu_{\bar{\nu}_e} \leq 2.7 \times 10^{-10} \mu_B$
ROVNO	$\mu_{\bar{\nu}_e} \leq 1.9 \times 10^{-10} \mu_B$
MUNU	$\mu_{\bar{\nu}_e} \leq 1.2 \times 10^{-10} \mu_B$
TEXONO	$\mu_{\bar{\nu}_e} \leq 2.0 \times 10^{-10} \mu_B$
Accelerators	
LAMPF	$\mu_{\nu_e} \leq 7.3 \times 10^{-10} \mu_B$
LAMPF	$\mu_{\nu_\mu} \leq 5.1 \times 10^{-10} \mu_B$
LSND	$\mu_{\nu_e} \leq 1.0 \times 10^{-9} \mu_B$
LSND	$\mu_{\nu_\mu} \leq 6.5 \times 10^{-10} \mu_B$

Table 1: 90% C.L. limits (95% C.L. for Rovno) on the effective NMM from reactor and accelerator data.

Limits on the effective NMM from Borexino data

Experiment.	Previous limit [9]	This work
Borexino	$\mu_\nu \leq 5 \times 10^{-11} \mu_B$	$\mu_\nu \leq 3.1 \times 10^{-11} \mu_B$

Table 2: 90% C.L. limits on the effective NMM from Borexino data. We show for comparison the constraint previously reported and the bound obtained in this work.

[9] C. Arpesella, et al., Phys. Rev. Lett. 101 (2008) 091302.

Experiment.	$\|\Lambda_1\|$	$\|\Lambda_2\|$	$\|\Lambda_3\|$
KRASNO	$4.7 \times 10^{-10}\mu_B$	$3.3 \times 10^{-10}\mu_B$	$2.8 \times 10^{-10}\mu_B$
ROVNO	$3.0 \times 10^{-10}\mu_B$	$2.1 \times 10^{-10}\mu_B$	$1.8 \times 10^{-10}\mu_B$
MUNU	$2.1 \times 10^{-10}\mu_B$	$1.5 \times 10^{-10}\mu_B$	$1.3 \times 10^{-10}\mu_B$
TEXONO	$3.4 \times 10^{-10}\mu_B$	$2.4 \times 10^{-10}\mu_B$	$2.0 \times 10^{-10}\mu_B$
GEMMA	$5.0 \times 10^{-11}\mu_B$	$3.5 \times 10^{-11}\mu_B$	$2.9 \times 10^{-11}\mu_B$
LSND	$6.0 \times 10^{-10}\mu_B$	$8.1 \times 10^{-10}\mu_B$	$7.0 \times 10^{-10}\mu_B$
LAMPF	$4.5 \times 10^{-10}\mu_B$	$6.2 \times 10^{-10}\mu_B$	$5.3 \times 10^{-10}\mu_B$
Borexino	$5.6 \times 10^{-11}\mu_B$	$4.0 \times 10^{-11}\mu_B$	$3.1 \times 10^{-11}\mu_B$

Table 3: 90% C.L. limits on the NMM components in the mass basis, Λ_i, from reactor, accelerator, and solar data from Borexino. In this particular analysis we constrain one parameter at a time, setting all other magnetic moment parameters and phases to zero.

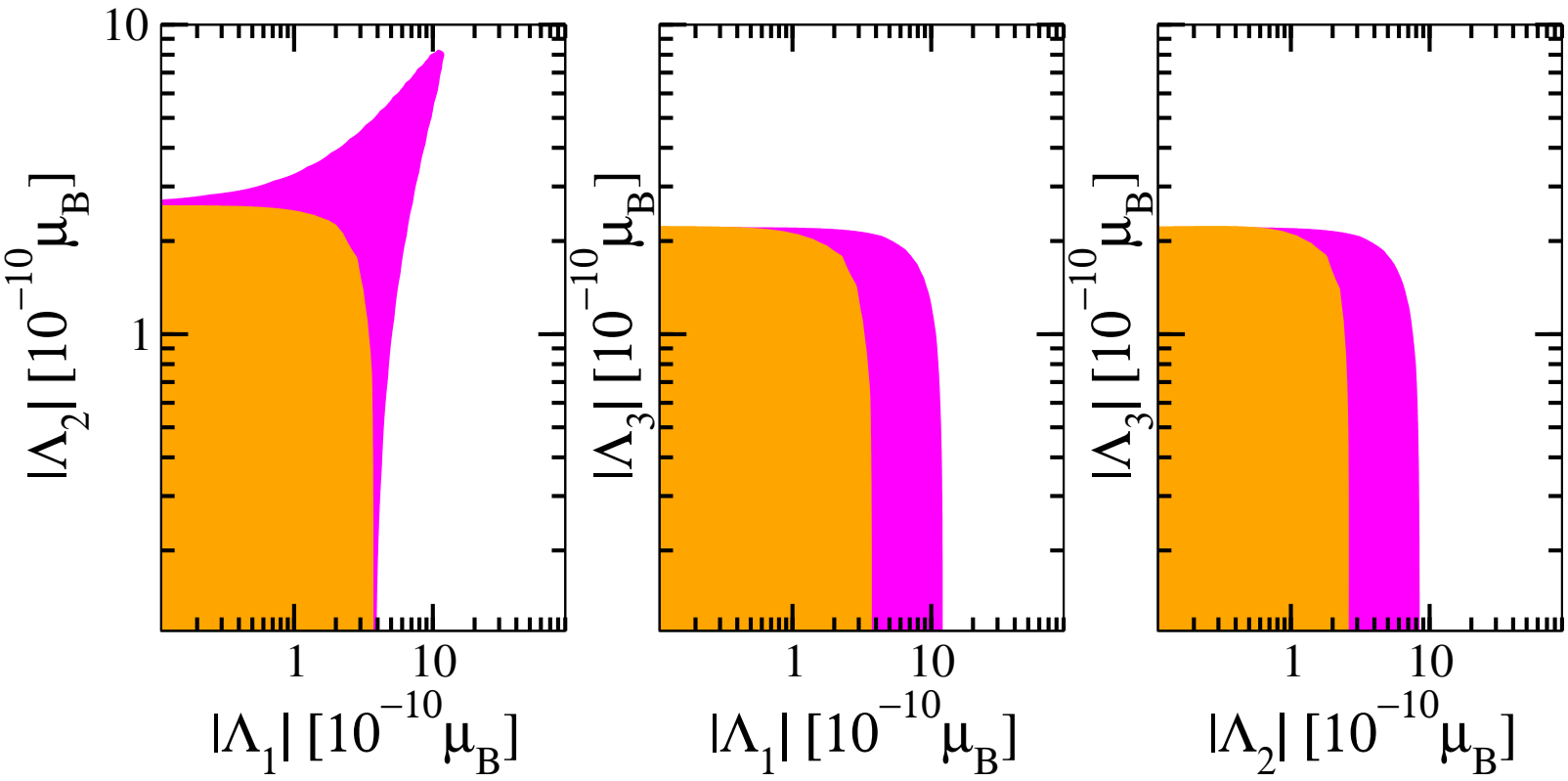

Figure 3: 90% C.L. allowed regions for the TNMMs in the mass basis from the reactor experiment TEXONO. The two-dimensional projections in the plane ($|\Lambda_i|$, $|\Lambda_j|$) have been calculated marginalizing over the third component. The magenta (outer) region is obtained for $\delta = 3\pi/2$ and $\xi_2 = \xi_3 = 0$, while the orange (inner) region appears for $\delta = 3\pi/2$, $\xi_2 = 0$ and $\xi_3 = \pi/2$.

Combined analysis

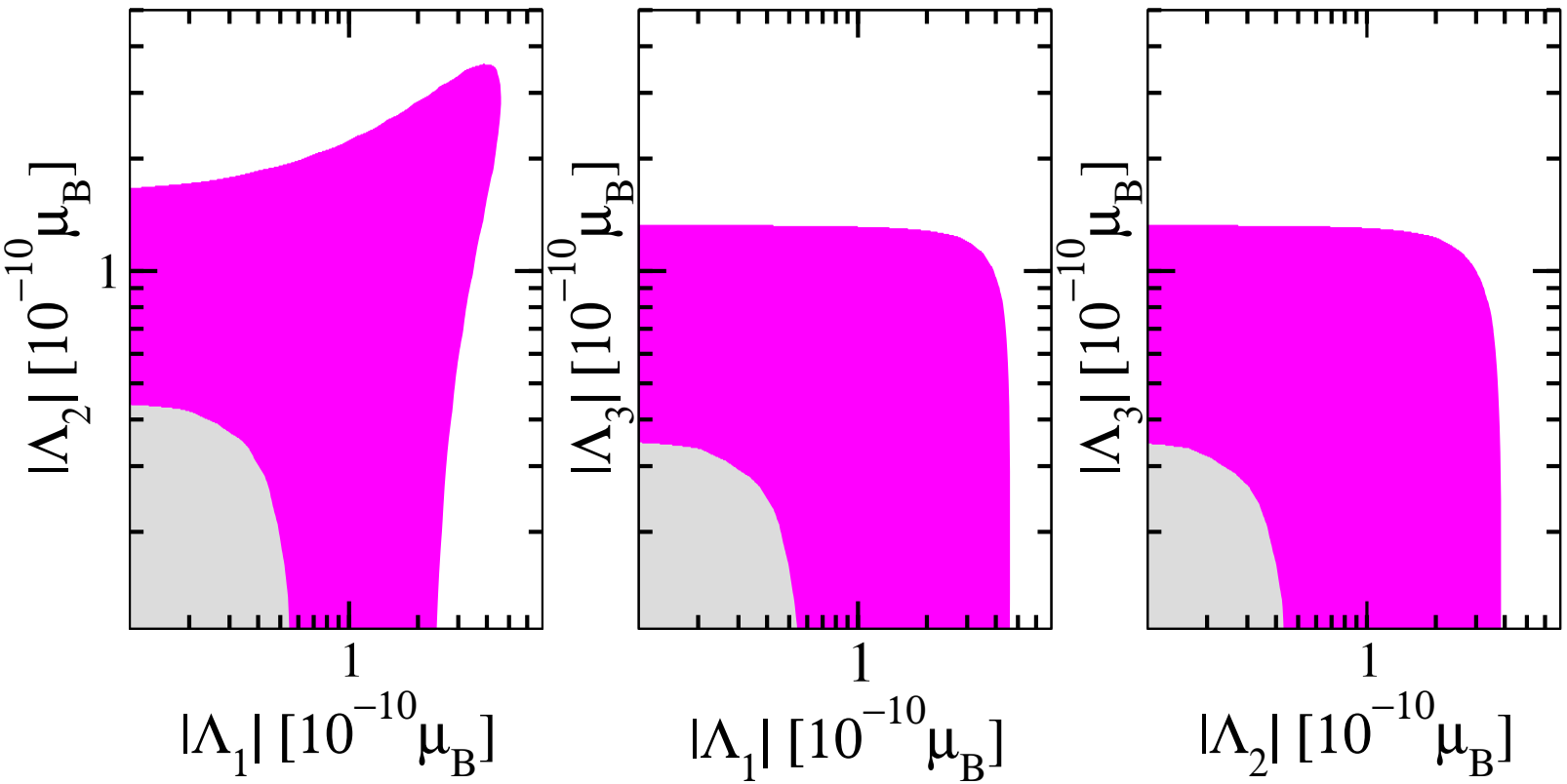

Figure 4: 90% C.L. allowed regions for the TNMMs in the mass basis. The result of this plot was obtained for the two parameters $|\Lambda_i|$ vs $|\Lambda_j|$ marginalizing over the third component. We show the result of a combined analysis of reactor and accelerator data with all phases set to zero except for $\delta = 3\pi/2$ (magenta region). We also show the result of the Borexino data analysis only, that is phase-independent (grey region). It is visible that Borexino data gives a more stringent constraint.

Conclusions

- ✓ In this work we have analyzed the current status of the constraints on NMMs. We have presented a detailed discussion of the constraints on the absolute value of the TMMs, as well as the role of the CP phases, stressing the complementarity of different experiments.
- ✓ Thanks to the low energies observed, below 1 MeV, and its robust statistics, the Borexino solar experiment plays a very important role in constraining the electromagnetic neutrino properties.
  Indeed, it provides stringent constraints on the absolute magnitude of the the TMMs, which we obtain as

$$
\begin{aligned}
|\Lambda_1| &\leq 5.6 \times 10^{-11} \mu_B \,, \\
|\Lambda_2| &\leq 4.0 \times 10^{-11} \mu_B \,, \\
|\Lambda_3| &\leq 3.1 \times 10^{-11} \mu_B \,.
\end{aligned}
$$

- ✓ However, the incoherent nature of the solar neutrino flux makes Borexino insensitive to the Majorana phases which characterize the transition moments matrix.
- ✓ Although less sensitive to the absolute value of the transition magnetic moment strengths, reactor and accelerator experiments provide the only chance to obtain a hint of the complex CP phases. We illustrate this fact by presenting the constraints resulting from our global analysis for different values of the relevant CP phases.
- ✓ Indeed, as we have illustrated, improved reactor and accelerator neutrino experiments will be crucial towards obtaining the detailed structure of the neutrino electromagnetic properties.

Thank you